

1 LEVERAGING MULTI-MESSENGER ASTROPHYSICS FOR DARK MATTER SEARCHES

By

Daniel Nicholas Salazar-Gallegos

A DISSERTATION

Submitted to
Michigan State University
in partial fulfillment of the requirements
for the degree of

Physics—Doctor of Philosophy
Computational Mathematics in Science and Engineering—Dual Major

Today

ABSTRACT

3 I did Dark Matter with HAWC and IceCube. I also used Graph Neural Networks

⁴ Copyright by

⁵ DANIEL NICHOLAS SALAZAR-GALLEGOS

⁶ Today

ACKNOWLEDGMENTS

8 I love my friends. Thanks to everyone that helped me figure this out. Amazing thanks to the people
9 at LANL who supported me. Eames, etc Dinner Parties Jenny and her child Kaydince Kirsten, Pat,
10 Andrea Family. You're so far but so critical to my formation. Unconditional love. Roommate

TABLE OF CONTENTS

12	LIST OF TABLES	vi
13	LIST OF FIGURES	vii
14	LIST OF ABBREVIATIONS	ix
15	CHAPTER 1 INTRODUCTION	1
16	CHAPTER 2 DARK MATTER IN THE COSMOS	2
17	2.1 Introduction	2
18	2.2 Dark Matter Basics	3
19	2.3 Evidence for Dark Matter	4
20	2.4 Searching for Dark Matter	11
21	2.5 Sources for Indirect Dark Matter Searches	16
22	2.6 Multi-Messenger Dark Matter	18
23	CHAPTER 3 MULTIMESSENGER ASTROPHYSICS: DETECTING HIGH EN-	
24	ERGY NEUTRAL MESSENGERS	21
25	3.1 Introduction	21
26	3.2 Charged Particles in a Medium	21
27	3.3 Photons (γ)	22
28	3.4 Neutrinos (ν)	22
29	3.5 Opportunities to Combine for Dark Matter	22
30	CHAPTER 4 HIGH ALTITUDE WATER CHERENKOV (HAWC) OBSERVATORY .	24
31	4.1 The Detector	24
32	4.2 Events Reconstruction and Data Acquisition	24
33	4.3 Remote Monitoring	24
34	CHAPTER 5 ICECUBE NEUTRINO OBSERVATORY	25
35	5.1 The Detector	25
36	5.2 Events Reconstruction and Data Acquisition	25
37	5.3 Northern Test Site	25
38	CHAPTER 6 COMPUTATIONAL TECHNIQUES IN PARTICLE ASTROPHYSICS .	26
39	6.1 Neural Networks for Gamma/Hadron Separation	26
40	6.2 Parallel Computing for Dark Matter Analyses	26
41	CHAPTER 7 GLORY DUCK	27
42	CHAPTER 8 NU DUCK	28
43	BIBLIOGRAPHY	29

44

LIST OF TABLES

45 Proof I know how to include

LIST OF FIGURES

47	Figure 2.1	Rotation curve fit to NGC 6503 from [7]. Dashed line is the contribution 48 from visible matter. Dotted curves are from gas. Dash-dot curves are from 49 dark matter (DM). Solid line is the composite contribution from all matter 50 and DM sources. Data are indicated with bold dots with error bars. Data 51 agree strongly with matter + DM composite prediction	5
52	Figure 2.2	Light from distant galaxy is bent in unique ways depending on the distribution 53 of mass between the galaxy and Earth. Yellow dashed lines indicate where 54 the light would have gone if the matter were not present [8].	7
55	Figure 2.3	(left) Optical image of galactic cluster. (right) X-ray image of the cluster with 56 redder meaning hotter and higher baryon density. (both) Green contours are 57 reconstruction of gravity contours from micro-lensing. White rings are the 58 best fit mass maxima at 68.3%, 95.5%, and 99.7% confidence. The maxima 59 of the clusters are clearly separated from x-ray maxima. [10]	8
60	Figure 2.4	Plank CMB sky. Sky map features small variations in temperature in pri- 61 mordial light. These anisotropies can be used to make inferences about the 62 universe's energy budget. [11]	9
63	Figure 2.5	Observed Cosmic Microwave Background power spectrum as a function of 64 multipole momentfrom Plank [11]. Blue line is best fit model from Λ CDM. 65 Red points and lines are data and error respectively.	10
66	Figure 2.6	Predicted power spectra of CMB for different $\Omega_m h^2$ values. (left) Low $\Omega_m h^2$ 67 increases the prominence of first and second peaks. (middle) $\Omega_m h^2$ is most 68 similar to the observed power spectrum. The second and third peaks are 69 similar in height. (right) $\Omega_m h^2$ is large which suppresses the first peak and 70 raises the prominence of the third peak.	10
71	Figure 2.7	The Standard Model (SM) of particle physics. Figure taken from http://www.quantumdiaries.org/2014/03/14/the-standard-model-a-beautiful-but-flawed-theory/	12
74	Figure 2.8	Simplified Feynman diagram demonstrating with different ways DM can 75 interact with SM particles. The 'X's refer to the DM particles whereas the 76 SM refer to fundamental particles in the SM. The large circle in the center 77 indicates the vertex of interaction and is purposely left vague. The colored 78 arrows refer to different directions of time as well as their respective labels. 79 The arrows indicate the initial and final state of the DM -SM interaction in time.	13

80	Figure 2.9 A single jet event in ATLAS detector from 2017 [16]. Jet momentum observed 81 to be 1.9 TeV. Missing transverse momentum observed to be 1.9 TeV as the 82 initial momentum of the event was 0. Implied MET is shown as a red dashed 83 line in event display.	14
84	Figure 2.10 More detailed pseudo-Feynman diagram of particle cascade from dark matter 85 annihilation into 2 quarks. The quarks hadronize and down to stable particles 86 like γ or the anti-proton (p^-). Diagram pulled from ICRC 2021 presentation 87 on DM annihilation search [17].	15
88	Figure 2.11 Dark Matter (DM) decay spectrum for $b\bar{b}$ initial state and γ final state. Redder 89 spectra are for larger DM masses. Bluer spectra are light DM masses. x is a 90 unitless factor defined as the ratio of the mass of DM, m_χ , and the final state 91 particle energy E_γ . Figure from [19].	17
92	Figure 2.12 Different dark matter density profiles compared. Some models produce very 93 large densities at small r [20].	18
94	Figure 2.13 The Milky Way Galaxy in photons (γ) and neutrinos (ν) [22]. Galactic center 95 is at $l=0^\circ$ and is the brightest region in all panels. (top) An Optical color image 96 of the Milky Way galaxy seen from Earth. Clouds of gas and dust obscure 97 some of the light from stars. (2nd down) Integrated flux of γ -rays observed 98 by the Fermi-LAT telescope [23]. (middle) Expected neutrino emmision 99 that corresponds with Fermi-LAT observations. (2nd up) Expected neutrino 100 emmision profile after considering detector systematics of IceCube. (bottom) 101 Observed neutrino emmision from region of the galactic plane. Substantial 102 neutrino emmision is detected.	19
103	Figure 2.14 Dark Matter annihilation spectra for different final state particle and standard 104 model annihilation channels [24]. Photons (red), e^\pm (green), \bar{p} (blue), ν (black).	20
105	Figure 3.1 TODO: Show a nuclear reactor with cherenkov radiation[NEEDS A SOURCE][FACT 106 CHECK THIS]	22
107	Figure 3.2 TODO: absorption spectrum of liquid and solid water[NEEDS A SOURCE][FACT 108 CHECK THIS]	23

LIST OF ABBREVIATIONS

- 110 **MSU** Michigan State University
111 **LANL** Los Alamos National Laboratory
112 **DM** Dark Matter
113 **SM** Standard Model
114 **HAWC** High Altitude Water Cherenkov Observatory

115

CHAPTER 1

INTRODUCTION

116 Is the text not rendering right? Ah ok it knows im basically drafting the doc still

CHAPTER 2

117

DARK MATTER IN THE COSMOS

118 **2.1 Introduction**

119 I will attempt to explain the dark matter problem at an entry level with the following thought
120 experiment. Imagine you are the teacher for an elementary school classroom. You take them on a
121 field trip to your local science museum and among the exhibits is one for mass and weight. The
122 exhibit has a gigantic scale, and you produce a fun problem for your classroom.

123 You ask your class, "What is the total weight of the classroom? Give your best estimation to
124 me in 30 minutes, and then we'll check your guess on the scale. If your guess is within 10% of the
125 right answer, we will stop for ice cream on the way back"

126 The students are ecstatic to hear this, and they get to work. The solution is some variation of
127 the following strategy. The students should give each other their weight or best guess if they do
128 not know. Then, all they must do is add each student's weight and get a grand total for the class.
129 The measurement on the giant scale should show the true weight of the class. When comparing the
130 measured weight, multiply the observation by 1.1 and 0.9 to get the +/- 10% tolerance, respectively.

131 Two of your students, Sandra and Mario, return to you with a solution.

132 They say, "We weren't sure of everyone's weight. We used 65 lbs. for the people we didn't
133 know and added everyone who does know. There are 30 of us, and we got 2,000 lbs.! That's a ton!"

134 You estimated 1,900 lbs. assuming the average weight of a student in your class was 60 lbs.
135 So, you are pleased with Sandra's and Mario's answer. You instruct your students to all gather on
136 the giant scale and read off the weight together. To all your surprise, the scale reads *10,000 lbs.!*
137 10,000 is significantly more than a 10% error from 2,000. In fact, it is approximately 5 times more
138 massive than either your or your students' estimates. You think to yourself and conclude there
139 must be something wrong with the scale. You ask an employee to check the scale and verify it is
140 calibrated well. They confirm that the scale is in working order. You weigh a couple of students
141 individually to test that the scale is well calibrated. Sandra weighs 59 lbs., and Mario weighs 62
142 lbs., typical weights for their age. You then weigh each student individually and see that their

143 weights individually do not deviate greatly from 60 lbs. So, where does all the extra weight come
144 from?

145 This thought experiment serves as an analogy to the Dark Matter problem. The important
146 substitution to make however is to replace the students with stars and the classroom with a galaxy,
147 say the Milky Way. Individually the mass of stars is well measured and defined with the Sun as our
148 nearest test case. However, when we set out to measure the mass of a collection of stars as large as
149 galaxies, our well-motivated estimation is wildly incorrect. There simply is no way to account for
150 this discrepancy except without some unseen, or dark, contribution to mass and matter in galaxies.
151 I set out in my thesis to narrow the possibilities of what this Dark Matter could be.

152 This chapter is organized like the following... **TODO: Text should look like ... Chaper x has**
153 **blah blah blah.**

154 2.2 Dark Matter Basics

155 Presently, the most compelling Dark Matter (DM) model is Λ Cold Dark Matter, or Λ CDM. I
156 present the evidence supporting Λ CDM in 2.3, yet discuss the conclusions of the Λ CDM model
157 here. According to Λ CDM fit to observations on the Cosmic Microwave Background (CMB), DM
158 is 26.8% of the universe's current energy budget Baryonic matter, stuff like atoms, gas, and stars,
159 contributes to 4.9% of the universe's current energy budget [1, 2, 3].

160 DM is dark; it does not interact readily with light at any wavelength. DM also does not interact
161 noticeably with the other standard model forces (Strong and Weak) at a rate that is readily observed
162 [3]. DM is cold, which is to say that the average velocity of DM is below relativistic speeds [1].
163 'Hot' DM would not likely manifest the dense structures we observe like galaxies, and instead
164 would produce much more diffuse galaxies than what is observed [3, 1]. DM is old; it played a
165 critical role in the formation of the universe and the structures within it [1, 2].

166 Observations of DM have so far been only gravitational. The parameter space available to
167 what DM could be therefore is extremely broad. Searches for DM are summarized by supposing
168 a hypothesis that has not yet been ruled out and performing measurements to test them. When
169 the observations yield a null result, the parameter space is further constrained. I present some

170 approaches for DM searches in Section 2.4.

171 **2.3 Evidence for Dark Matter**

172 Dark Matter (DM) has been a looming problem in physics for almost 100 years. Anomalies
173 have been observed in galactic dynamics as early as 1933 when Fritz Zwicky noticed unusually
174 large velocity dispersions in the Coma cluster. Zwicky's measurement was the first recorded to
175 use the Virial theorem to measure the mass fraction of visible and invisible matter in celestial
176 bodies [4]. From Zwicky in [5], "*If this would be confirmed, we would get the surprising result*
177 *that dark matter is present in much greater amount than luminous matter.*" Zwicky's and others'
178 observation did not instigate a crisis in astrophysics because the measurements did not entirely
179 conflict with their understanding of galaxies [4]. In 1978, Rubin, Ford, and Norbert measured
180 rotation curves for ten spiral galaxies [6]. Rubin et. al.'s 1978 publication presented a major
181 challenge to the conventional understanding of galaxies that could no longer be accredited to
182 measurement uncertainties. Evidence has been mounting ever since for this exotic form of matter.
183 The following subsections sample some of the compelling evidence supporting DM.

184 **2.3.1 First Clues: Stellar Velocities**

185 Zwicky's, and later Rubin's, measurements of the stellar velocities were built upon the Virial
186 theorem, shown as

$$2T + V = 0. \quad (2.1)$$

187 Where T is the kinetic energy and V is the potential energy in a self-gravitating system. The
188 potential was defined as the classical Newton's law of gravity from stars and gas contained in the
189 observed galaxies

$$V = -\frac{1}{2} \sum_i \sum_{j \neq 1} \frac{m_i m_j}{r_{ij}}. \quad (2.2)$$

190 Zwicky et. al. measured just the velocities of stars apparent in optical wavelengths [5]. Rubin et.
191 al. added by measuring the velocity of the hydrogen gas via the 21 cm emission line of Hydrogen
192 [6]. The velocities of the stars and gas are used to infer the total mass of galaxies and galaxy clusters
193 via Eq. (2.1). An inferred mass is also made from the luminosity of the selected sources. The two

194 inferences are compared to each other as a luminosity to mass ratio and typically yields [1]

$$\frac{M}{L} \sim 400 \frac{M_{\odot}}{L_{\odot}} \quad (2.3)$$

195 M_{\odot} and L_{\odot} referring to stellar mass and stellar luminosity, respectively. These ratios clearly indicate
196 a discrepancy in apparent light and mass from stars and gas and their velocities.

197 Rubin et.al. [6] demonstrated that the discrepancy was unlikely to be an under-estimation of
198 the mass of the stars and gas. The inferred 'dark' mass was up to 5 times more than the luminous
199 mass. This dark mass also needed to extend well beyond the extent of the luminous matter.

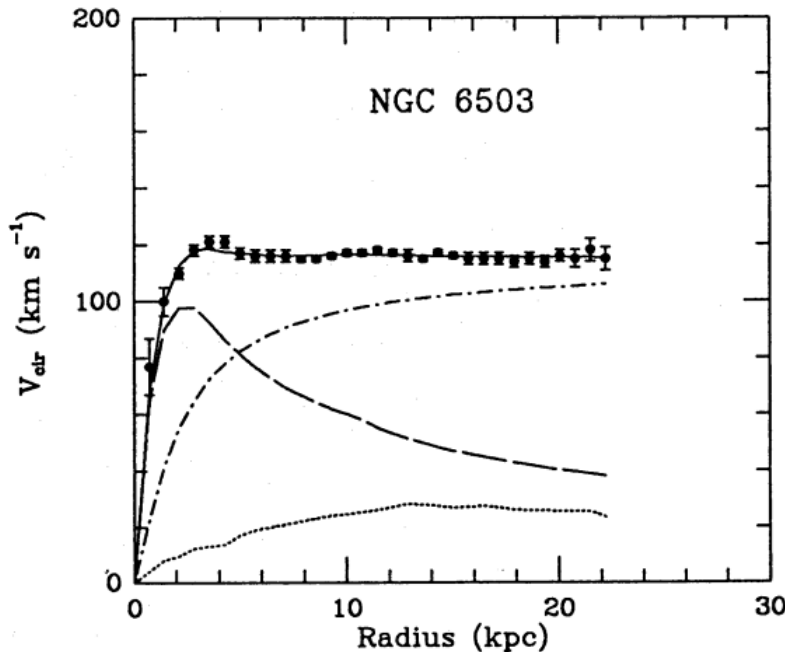


Figure 2.1 Rotation curve fit to NGC 6503 from [7]. Dashed line is the contribution from visible matter. Dotted curves are from gas. Dash-dot curves are from dark matter (DM). Solid line is the composite contribution from all matter and DM sources. Data are indicated with bold dots with error bars. Data agree strongly with matter + DM composite prediction

200 Fig. 2.1: features one of many observations made on the stellar velocities within galaxies.
201 The measured rotation curves mostly feature a flattening of velocities at higher radius which is
202 not expected if the gravity was only coming from gas and luminous matter. The extension of
203 the flat velocity region also indicates that the DM is distributed far from the center of the galaxy.
204 Modern velocity measurements include significantly larger objects, galactic clusters, and smaller

205 objects, dwarf galaxies. Yet, measurements along this regime are leveraging the Virial theorem
206 with Newtonian potential energies. We know Newtonian gravity is not a comprehensive description
207 of gravity. New observational techniques have been developed since 1978, and those are discussed
208 in the following sections.

209 **2.3.2 Evidence for Dark Matter: Micro-lensing**

210 Modern evidence for dark matter comes from new avenues beyond stellar velocities. Gravita-
211 tional micro-lensing from DM is a new channel from general relativity. The Cosmic Microwave
212 Background shows that the universe had DM in it from an incredibly early stage. Computational
213 resources have expanded in recent decades enabling universe models that again support the need
214 for DM in the evolution of the universe.

215 General relativity predicts aberrations in light caused by massive objects. In recent decades
216 we have been able to measure the lensing effects from compact objects and DM haloes. Fig. 2.2
217 shows how different compact bodies change the final image of a faraway galaxy resulting from
218 gravitational lensing. Gravitational lensing developed our understanding of dark matter in two
219 important ways.

220 First, micro-lensing observations, or the lack of them, of our Milky Way halo resulted in a
221 conspicuous absence of massive astrophysical compact halo objects (MACHOs). The hypothesis
222 was that 'dark matter' could be accounted for by sufficiently dim compact objects. Such objects
223 include things like planets, brown dwarves, black holes, or neutron stars. Whenever these objects
224 passed in front of a large luminous source, such as the Large Magelenic Clouds, a variation in light
225 should be observed [4]. The MACHO and EROS collaborations performed this observation and
226 did not find a substantial contribution to the DM Milky Way halo from MACHOs. They measured
227 that MACHOs of mass range 0.15 to $0.9 M_{\odot}$ contributes to an upper limit of 8% of the DM halo
228 mass [9].

229 Gravitational lensing can also be applied towards galaxy clusters for DM searches. The obser-
230 vation of two merging galactic clusters in 2006, shown in Fig. 2.3, provided a compelling argument
231 for particle DM outside the Standard Model. These clusters merged recently in astrophysical time

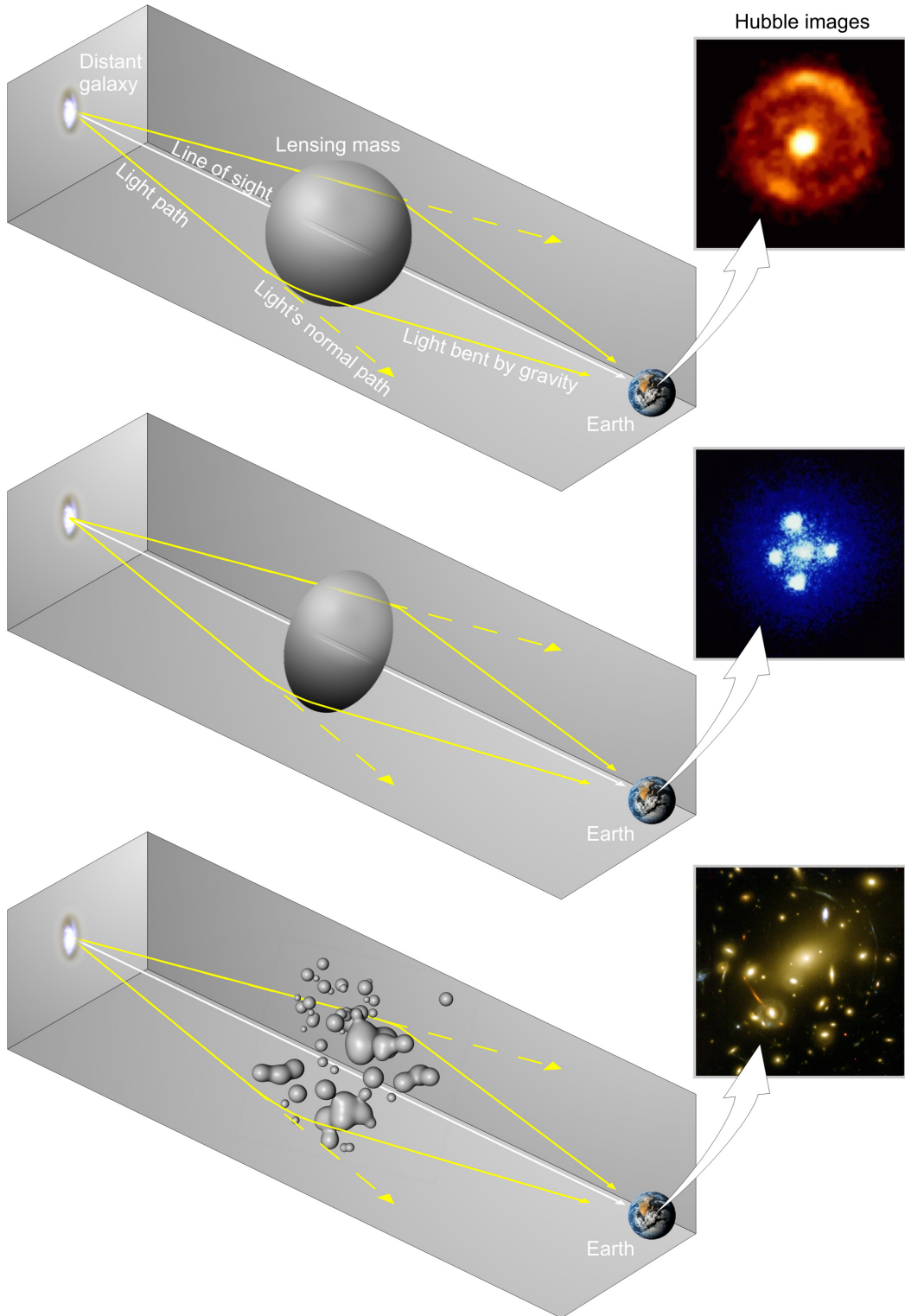


Figure 2.2 Light from distant galaxy is bent in unique ways depending on the distribution of mass between the galaxy and Earth. Yellow dashed lines indicate where the light would have gone if the matter were not present [8].

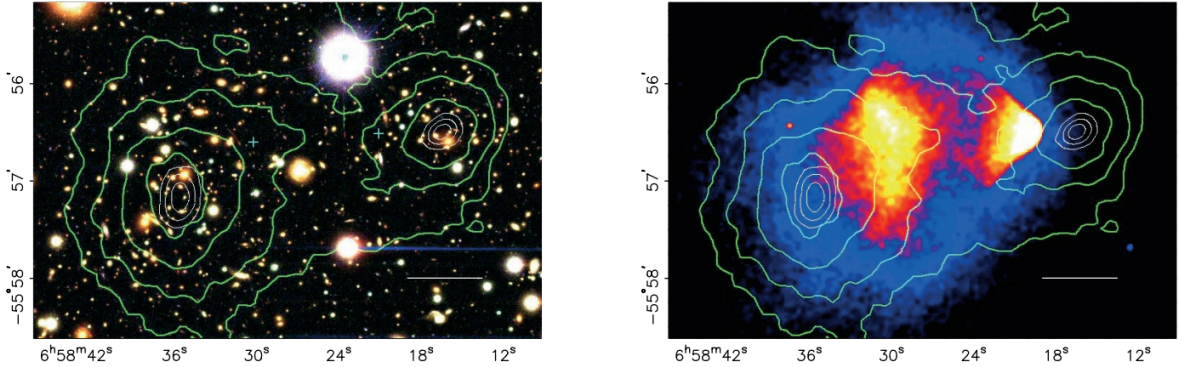


Figure 2.3 (left) Optical image of galactic cluster. (right) X-ray image of the cluster with redder meaning hotter and higher baryon density. (both) Green contours are reconstruction of gravity contours from micro-lensing. White rings are the best fit mass maxima at 68.3%, 95.5%, and 99.7% confidence. The maxima of the clusters are clearly separated from x-ray maxima. [10]

232 scales. Their recent merger separated the stars and galaxies are separated from the intergalactic
 233 gas. For these clusters, the hot, intergalactic gas is responsible for most of the mass in the systems
 234 [4]. The hot gas is observed from its x-rays argument. Two observations of the clusters were made
 235 independently of each other. The first was the microlensing of light around the galaxies due to
 236 their gravitational influences. When celestial bodies are large enough, the gravity they exert bends
 237 space and time itself. These bending effects light and will deflect light an analogous way to how
 238 lenses will bend light. With a sufficient understanding of light sources behind a celestial body, we
 239 can reconstruct the contours of the gravitational lenses. The gradient of the contours then indicates
 240 how dense the matter is and where it is.

241 The x-ray emission can then be observed from the clusters. Since these galaxies are mostly gas
 242 and are merging, then the gas should be getting hotter. If they are merging, the x-ray emissions
 243 should be the strongest where the gas is mostly moving through each other. Hence, X-ray emission
 244 maps out where the gas is in the merging galaxy cluster.

245 The micro-lensing and x-ray observations were done on the Bullet cluster featured on Fig. 2.3.
 246 The x-ray emmisions does not align with the gravitational countours from microlensing. The
 247 incongruence in mass density and baryon density suggests that there is a lot of matter somewhere
 248 that does not interact with light. Moreover, this dark matter is can not be baryonic [10]. The Bullet

249 Cluster measurement did not really tell us what DM is exactly, but it did give the clue that DM also
250 does not interact with itself very strongly. If DM did interact strongly with itself, then it would
251 have been more aligned with the x-ray emmision [10]. There have been follow-up studies of galaxy
252 clusters with similar results. The Bullet Cluster and others like it provide a strong case against
253 something possibly amiss in our gravitational theories.

254 **2.3.3 Evidence for Dark Matter: Cosmic Microwave Background**

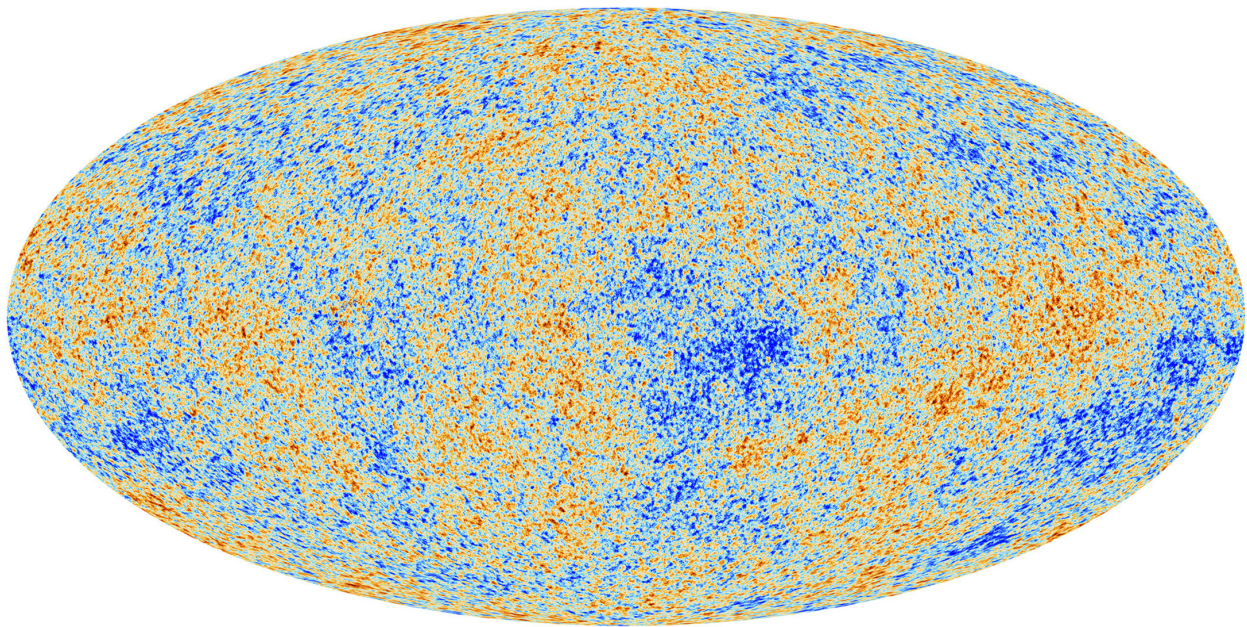


Figure 2.4 Plank CMB sky. Sky map features small variations in temperature in primordial light. These anisotropies can be used to make inferences about the universe's energy budget. [11]

255 The Cosmic Microwave Background (CMB) is the primordial light from the early universe
256 when Hydrogen atoms formed from the free electron and proton soup in the early universe. The
257 CMB is the earliest light we can observe; released when the universe was about 380,000 years old.
258 Then we look at how the simulated universes look like compared to what we see. Fig. 2.4 is the
259 most recent CMB image from the Plank observatory [11]. Redder regions indicate a slightly hotter
260 region of the early universe and blue indicates colder.

261 To measure the DM, Dark Energy, and matter fractions of the universe from the CMB, the image
262 is deconstructed into a power spectrum versus spherical multipole moments. Λ CDM provides the

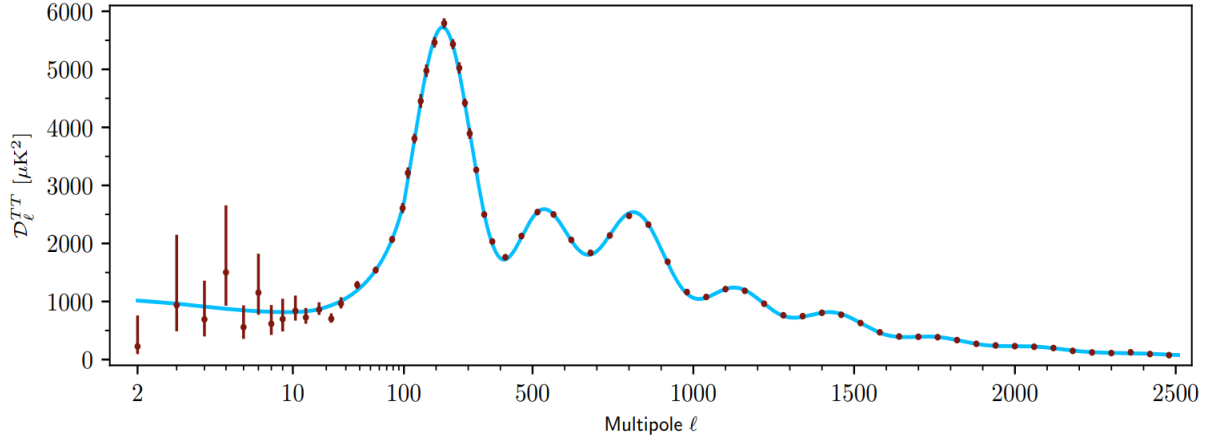


Figure 2.5 Observed Cosmic Microwave Background power spectrum as a function of multipole moment from Plank [11]. Blue line is best fit model from Λ CDM. Red points and lines are data and error respectively.

263 best fit to the power spectra of the CDM as shown in Fig. 2.5. The CMB power spectrum is very
 264 sensitive to the fraction of each energy contribution in the early universe. Low l modes are dominated
 265 by variations in gravitational potential. Intermediate l emerge from oscillations in photon-baryon
 266 fluid from competing baryon pressures and gravity. High l is a damped region from the diffusion
 267 of photons during electron-proton recombination. [1]

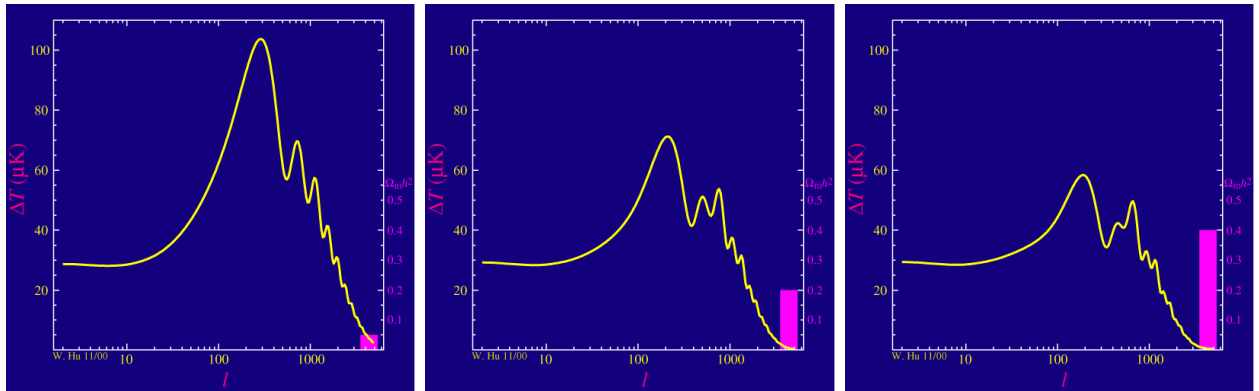


Figure 2.6 Predicted power spectra of CMB for different $\Omega_m h^2$ values. (left) Low $\Omega_m h^2$ increases the prominence of first and second peaks. (middle) $\Omega_m h^2$ is most similar to the observed power spectrum. The second and third peaks are similar in height. (right) $\Omega_m h^2$ is large which suppresses the first peak and raises the prominence of the third peak.

268 The harmonics would look very different for a universe with less DM. Fig. 2.6 shows the
 269 differences expected in the power spectrum for different baryon fractions of the universe's energy

270 budget. The observations fit well with the Λ CDM model and the derived fractions are as follows.
271 The matter fraction: $\Omega_m = 0.3153$; and the baryon fraction: $\Omega_b = 0.04936$ [11]. These findings
272 do rely however on a few assumptions and the precision of the Hubble constant, H_0 . H_0 especially
273 has seen a growing tension in recent decades that continues to deepened with observatories like the
274 James Webb Telescope [12, 13]

275 Overall these observations form a compelling body of research in favor of dark matter. However,
276 these observations really only confirm that DM is there. It takes another leap of theory and
277 experimentation to make observations of DM that are non-gravitational in nature. One hypothesis
278 is the Weakly Interacting Massive Particle DM. This DM candidate theory is discussed further in
279 the next section and is the hypothesis to this thesis.

280 **2.4 Searching for Dark Matter**

281 There remains many options available to what Dark Matter could be. For a particle dark matter
282 hypothesis, we assume that DM interacts in some way, even if very weakly, with the Standard
283 Model (SM), see Section 2.4. The current status of the SM does not have a viable DM candidate.
284 When looking at the standard model, we can immediately exclude any charged particle. This is
285 because charged particles interact with light. If DM is charged, it would be immediately visible if
286 it had similar charge to many SM particles. Specifically this will rule out the following charged,
287 fundamental particles: $e, \mu, \tau, W, u, d, s, c, t, b$ and their corresponding antiparticles. Recalling
288 from earlier that DM must be long lived and stable over the age of the universe, this would exclude
289 all SM particles with decay half-lives at or shorter than the age of the universe. The lifetime
290 constraint additionally eliminates the Z and H bosons. Finally, the candidate DM needs to be
291 somewhat massive. Recall from Section 2.2 that DM is cold or not relativistic through the universe.
292 This eliminates the remaining SM particles: $\nu_{e,\mu,\tau}, g, \gamma$ as DM candidates. Because there are no
293 DM candidates within the SM, the DM problem strongly hints to physics beyond the SM (BSM).

294 **2.4.1 Shake it, Break it, Make it**

295 When considering DM that couples in some way with the SM, the interactions are roughly
296 demonstrated by interaction demonstrated in Fig. 2.8. The figure is a simplified Feynman diagram

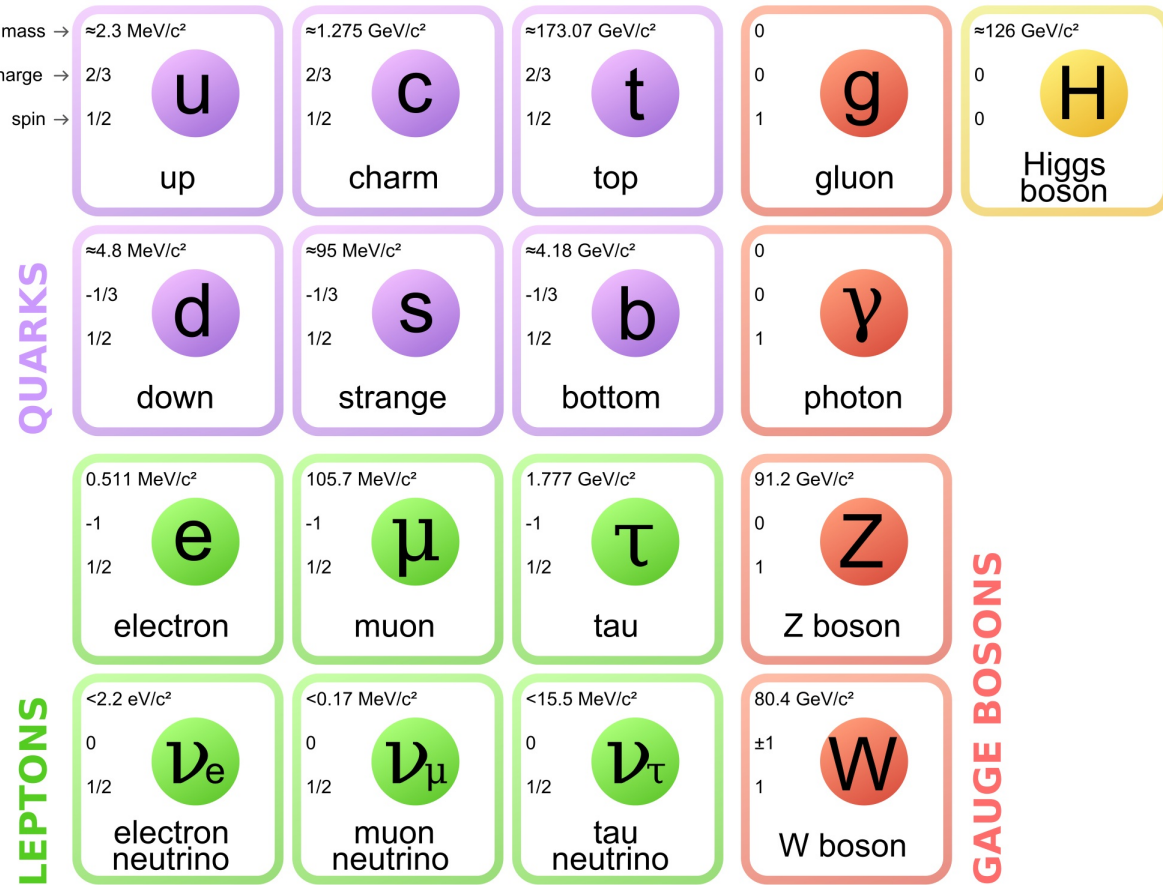


Figure 2.7 The Standard Model (SM) of particle physics. Figure taken from <http://www.quantumdiaries.org/2014/03/14/the-standard-model-a-beautiful-but-flawed-theory/>

- 297 where the arrow of time represents the interaction modes of: **Shake it, Break it, Make it.**
- 298 **Shake it** refers to the direct detection of dark matter. Direct detection interactions start with a
 299 free DM particle and some SM particle. The DM and SM interact under some elastic or inelastic
 300 collision and recoil away from each other. The DM remains in the dark sector and imparts some
 301 momentum onto the SM particle. The hope is that the momentum imparted onto the SM particle
 302 is sufficiently high enough to pick up with highly sensitive instruments. Because we cannot create
 303 the DM in the lab, a direct detection experiment must wait until DM is incident on the detector.
 304 Most direct detection experiments are therefore placed in low-background environments with inert
 305 detection media like the noble gas Xenon. [14]
- 306 **Make it** refers to the production of DM from SM initial states. The experiment starts with
 307 particles in the SM. These SM particles are accelerated to incredibly high energies and then collided

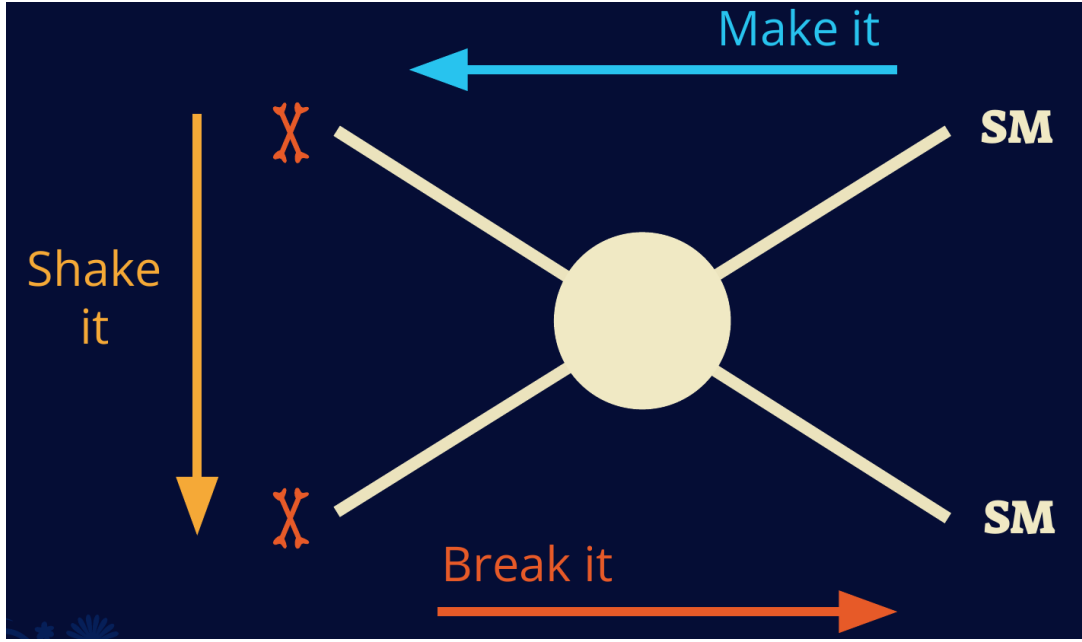


Figure 2.8 Simplified Feynman diagram demonstrating different ways DM can interact with SM particles. The 'X's refer to the DM particles whereas the SM refer to fundamental particles in the SM. The large circle in the center indicates the vertex of interaction and is purposely left vague. The colored arrows refer to different directions of time as well as their respective labels. The arrows indicate the initial and final state of the DM -SM interaction in time.

308 with each other. In the confluence of energy, DM hopefully emerges as a byproduct of the SM
 309 annihilation. Often it is the collider experiments that are able to generate energies high enough
 310 to probe DM production. These experiments include the world-wide collaborations ATLAS and
 311 CMS at CERN where protons are collided together at extreme energies. The DM searches however
 312 are complex. DM likely does not interact with the detectors and lives long enough to escape the
 313 detection apparatus of CERN's colliders. This means any DM production experiment searches for an
 314 excess of events with missing momentum or energy in the events. An example event with missing
 315 transverse momentum is shown in Fig. 2.9. The missing momentum with no particle tracks implies
 316 a neutral particle carried the energy out of the detector. However, there are other neutral particles
 317 in the SM, like neutrons or neutrinos, so any analysis have to account for SM signatures of missing
 318 momentum. [15]

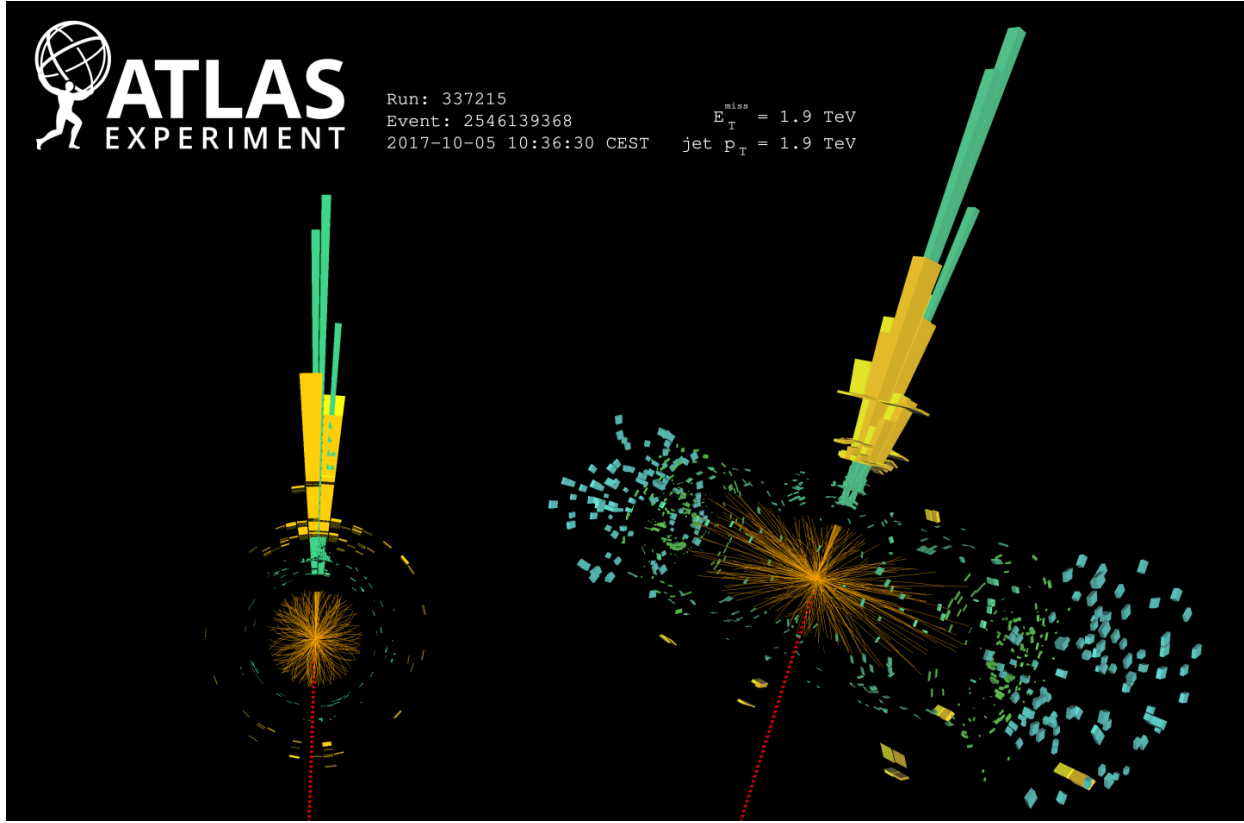


Figure 2.9 A single jet event in ATLAS detector from 2017 [16]. Jet momentum observed to be 1.9 TeV. Missing transverse momentum observed to be 1.9 TeV as the initial momentum of the event was 0. Implied MET is shown as a red dashed line in event display.

319 2.4.2 Break it: Standard Model Signatures of Indirect Dark Matter Searches

320 **Break it** refers to the creation of SM particles from the dark sector, and it is the primary focus
 321 of this thesis. The interaction begins with DM or in the dark sector. The hypothesis is that this
 322 DM will either annihilate with itself or decay and produce a SM byproduct. This method is often
 323 referred to the Indirect Detection of DM because we have no lab to directly control or manipulate the
 324 DM. Therefore most DM primary observations will be performed from observations of known DM
 325 densities among the astrophysical sources. The strength is that we have the whole of the universe
 326 and it's 13.6 billion year lifespan to use as the detector or particle accelerator. Additionally, locations
 327 of dark matter are also well understood since it was astrophysical observations that presented the
 328 problem of DM in the first place.

329 However, anything can happen in the universe. There are many difficult to deconvolve back-

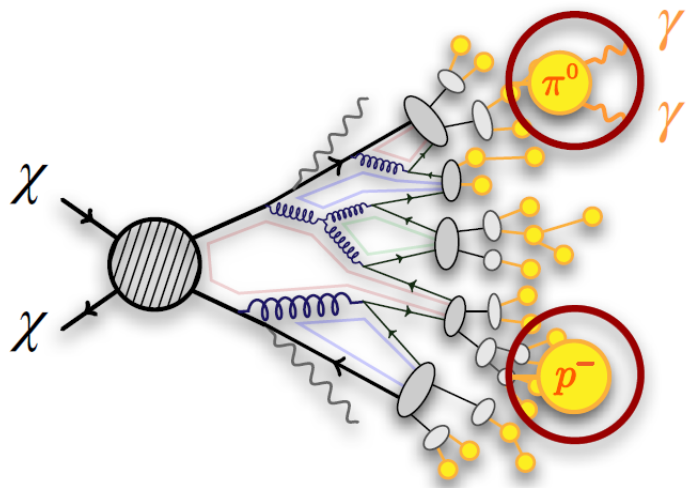


Figure 2.10 More detailed pseudo-Feynman diagram of particle cascade from dark matter annihilation into 2 quarks. The quarks hadronize and down to stable particles like γ or the anti-proton (p^-). Diagram pulled from ICRC 2021 presentation on DM annihilation search [17].

330 grounds when searching for DM. Once prominent example is the galactic center. There's a lot of
 331 DM there since the Milky Way definitely has a lot of DM. But any signal coming from there is hard
 332 to parse apart from the extreme environment of our supermassive black hole, Sagitarius A* [18]
 333 Despite the challenges, any DM model that yields evidence in the other observation two methods,
 334 **Shake it or Make it** must be corroborated with indirect observations of the known DM sources.
 335 Without corroborating evidence, DM observation in the lab is hard-pressed to demonstrate that it
 336 is the model contributing to the DM seen at the universal scale.

337 In the case of WIMP DM, signals are typically described in terms of primary SM particles
 338 produced from a DM decay or annihilation. The SM initial state particles are then simulated to
 339 stable final states such as the γ , ν , p , or e which can traverse galactic lengths to reach Earth.

340 Fig. 2.10 shows the quagmire of SM particles that emerges from SM initial states that are not
 341 stable [17]. There are many different particles with varying energies that can be produced in such an
 342 interaction. For any arbitrary DM source and stable SM particle, the SM flux from DM annihilating

343 to some neutral particle in the SM, ϕ , from a region in the sky is described by the following

$$\frac{d\Phi_\phi}{dE_\phi} = \frac{\langle\sigma v\rangle}{8\pi m_\chi^2} \frac{dN_\phi}{dE_\phi} \times \int_{\text{source}} d\Omega \int_{l.o.s} \rho_\chi^2 dl(r, \theta') \quad (2.4)$$

344 In Eq. (2.4), $\langle\sigma v\rangle$ is the velocity-weighted annihilation cross-section of DM to the SM. m_χ refers
345 to the mass of DM, noted with greek letter χ . $\frac{dN_\phi}{dE_\phi}$ is the N particle flux weighted by the particle
346 energy. An example is provided in Fig. 2.11 for the γ final state. The integrated terms are performed
347 over the solid angle, $d\Omega$, and line of sight, l.o.s. ρ is the density of DM for a location (r, θ') in the
348 sky. The terms left of the '×' are often referred to as the particle physics component. The terms on
349 the right are referred to as the astrophysical component. For decaying DM, the equation changes
350 to...

$$\frac{d\Phi_\phi}{dE_\phi} = \frac{1}{4\pi\tau m_\chi} \frac{dN_\phi}{dE_\phi} \times \int_{\text{source}} d\Omega \int_{l.o.s} \rho_\chi dl(r, \theta') \quad (2.5)$$

351 In Eq. (2.5), τ is the decay lifetime of the DM. Just as in Eq. (2.4), the left and right terms are
352 the particle physics and the astrophysical components respectively. The integrated astrophysical
353 component of Eq. (2.4) is often called the J-Factor. Whereas the integrated astrophysical component
354 of Eq. (2.5) is often called the D-Factor.

355 Exact DM $\text{DM} \rightarrow \text{SM}$ branching ratios are not known, so it is usually assumed to go 100%
356 into a SM particle/anti-particle. Additionally, when a DM annihilation or decay produces one of
357 the neutral, long-lived SM particles (ν or γ), the particle can be traced back to a DM source. For
358 DM above GeV energies, there are very few SM processes that can produce particles with such a
359 high energy. Seeing such a signal would almost certainly be an indication of the presence of dark
360 matter. The universe fortunately provides us with the largest volume and lifetime ever for a particle
361 physics experiment.

362 **2.5 Sources for Indirect Dark Matter Searches**

363 We of course have to know where to look. Thankfully, we have a good idea of where. The
364 first detection of DM relied on optical observations. Since then, we've developed new techniques
365 to find DM dense regions. As described in Section 2.3.1, many DM dense regions were through
366 observing galactic rotation curves. Our Milky Way galaxy is among DM dense regions discovered,

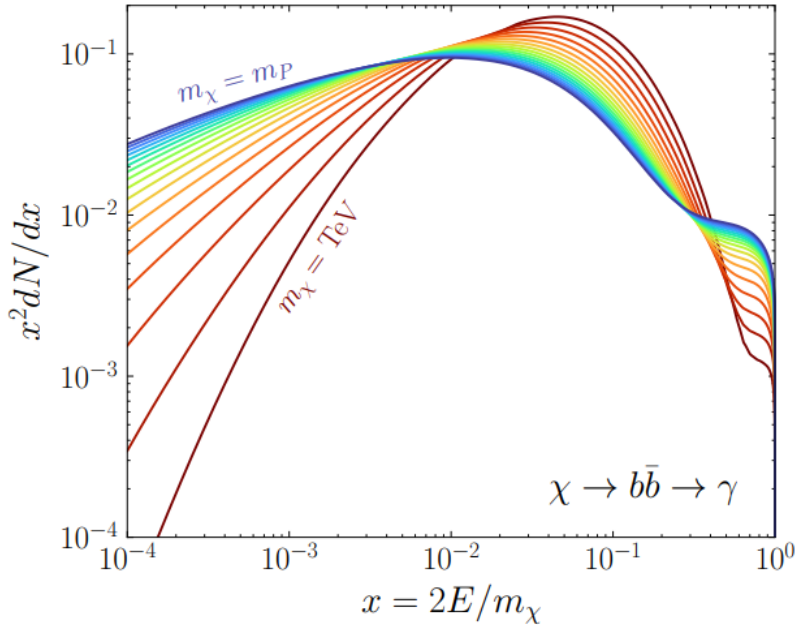


Figure 2.11 Dark Matter (DM) decay spectrum for $b\bar{b}$ initial state and γ final state. Redder spectra are for larger DM masses. Bluer spectra are light DM masses. x is a unitless factor defined as the ratio of the mass of DM, m_χ , and the final state particle energy E_γ . Figure from [19].

and it is the largest nearby DM dense region to look at. Additionally, the DM halo surrounding the Milky Way is somewhat clumpy [18]. There are regions in the DM halo of the Milky Way that have more DM than others they have captured gas over time. In some cases these sub-haloes were dense enough to host stars. These apparent sub galaxies are known was dwarf spheroidal galaxies and are the main sources studied in this thesis. Each source type comes with different trade offs. Galactic Center studies will be very sensitive to the assume distribution of DM. The central DM density can very substantially as demonstrated in Fig. 2.12. At small r, the differences in DM densities can be 3-4 orders of magnitude.

Dwarf Spheroidal Galaxies (dSph's) studies suffer from uncertainties in the DM density less than the galactic center studies. This is mostly from their diminutive size being smaller than the angular resolution of most γ -ray observatories [18]. The DM content dSph's are typically determined with the virial theorem, Eq. (2.1), and are usually majority DM [18] in mass. DSph's tend to be ideal sources to look at for DM searches. Their environments are fairly quiet with little

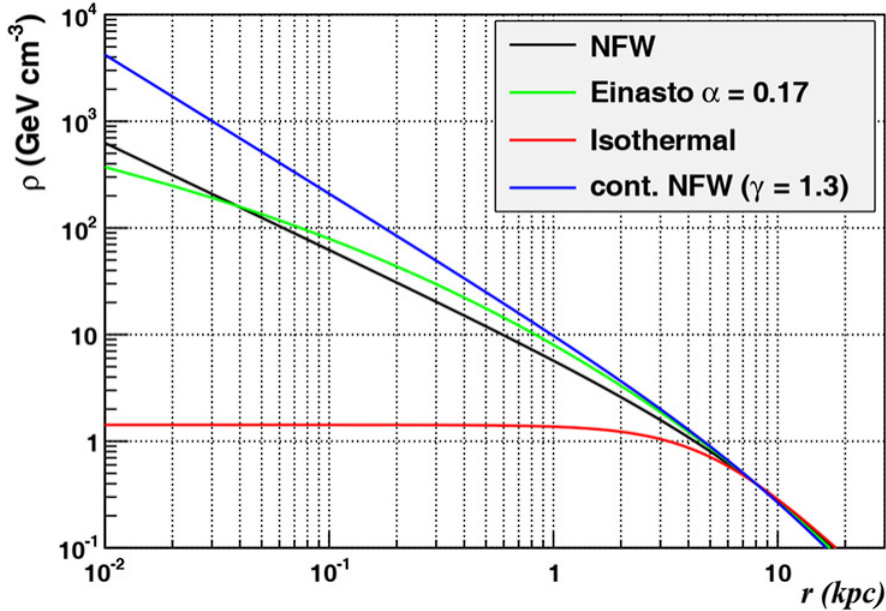


Figure 2.12 Different dark matter density profiles compared. Some models produce very large densities at small r [20].

380 astrophysical backgrounds. Unlike the galactic center, the most active components of dSph's are
 381 the stars within them versus a violent accretion disc around a black hole. All this together means
 382 that dSph's are among the best sources to look at for indirect DM searches. dSph's are the targets
 383 of focus for this thesis.

384 2.6 Multi-Messenger Dark Matter

385 Astrophysics entered a new phase in the past few decades that leverages our increasing sensitivity
 386 to SM channels and general relativity (GR). Up until the 21st century, astrophysical observations
 387 were done with photons (γ) only. Astrophysics with this 'messenger' is fairly mature now. Novel
 388 observations of the universe have since only adjusted the sensitivity of the wavelength of light
 389 that's observed. Gems like the CMB [11], and more have ultimately been observations of different
 390 wavelengths of light. Multi-messenger astrophysics proposes using other SM particles such the
 391 $p^{+/-}$, or ν or gravitation waves predicted by general relativity.

392 The experiments LIGO had a revolutionary discovery in 2016 with the first detection of a binary
 393 black hole merger [21]. This opened the collective imagination entirely to observing the universe

394 through gravitational waves. There's also been a surge of interest in the neutrino (ν) sector. IceCube
 395 demonstrated that we are sensitive to neutrinos in regions that correlate with significant photon
 396 emmission like the galactic plane [22]. Neutrinos, like gravitational waves and light, travel mostly
 397 unimpeded from their source to our observatories. This makes pointing to the oringinating source
 398 of the these messengers much easier than it is for cosmic rays that are almost always deflected from
 399 their source.

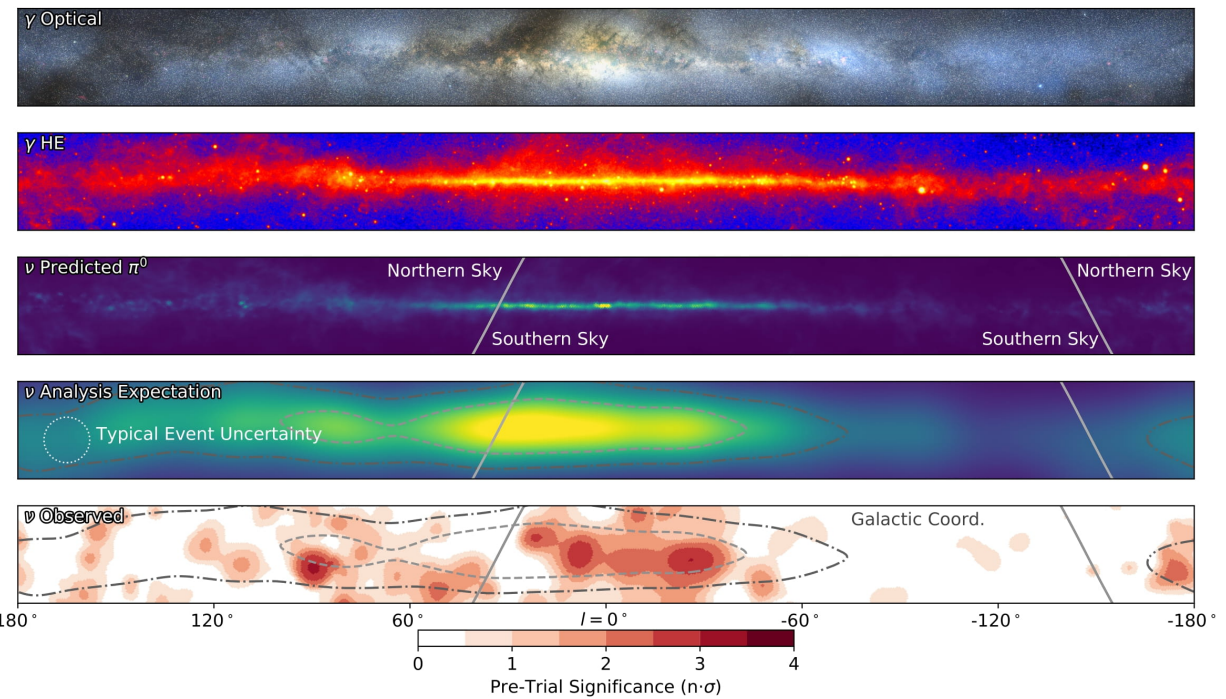


Figure 2.13 The Milky Way Galaxy in photons (γ) and neutrinos (ν) [22]. Galactic center is at $l=0^\circ$ and is the brightest region in all panels. (top) An Optical color image of the Milky Way galaxy seen from Earth. Clouds of gas and dust obscure some of the light from stars. (2nd down) Integrated flux of γ -rays observed by the Fermi-LAT telescope [23]. (middle) Expected neutrino emmision that corresponds with Fermi-LAT observations. (2nd up) Expected neutrino emmision profile after considering detector systematics of IceCube. (bottom) Observed neutrino emmision from region of the galactic plane. Substantial neutrino emmision is detected.

400 The recent result from IceCube, shown in Fig. 2.13, proves that we can make obervations under
 401 different messenger regimes. The top two panels are the appearance of the galactic plane to different
 402 wavelengths of light. Some sources are more apparent in some panels, while others are not. The
 403 IceCube collaboration recently published a groundbreaking result of the Milky Way in neutrinos.

404 This new channel is potentially very powerful because neutrinos are readily able to penetrate see
 405 through gas and dust in the Milky Way. This new image also refines our understanding of how high
 406 energy particles are accelerated since the fit to IceCube data prefers one standard model process
 407 over the other [22].

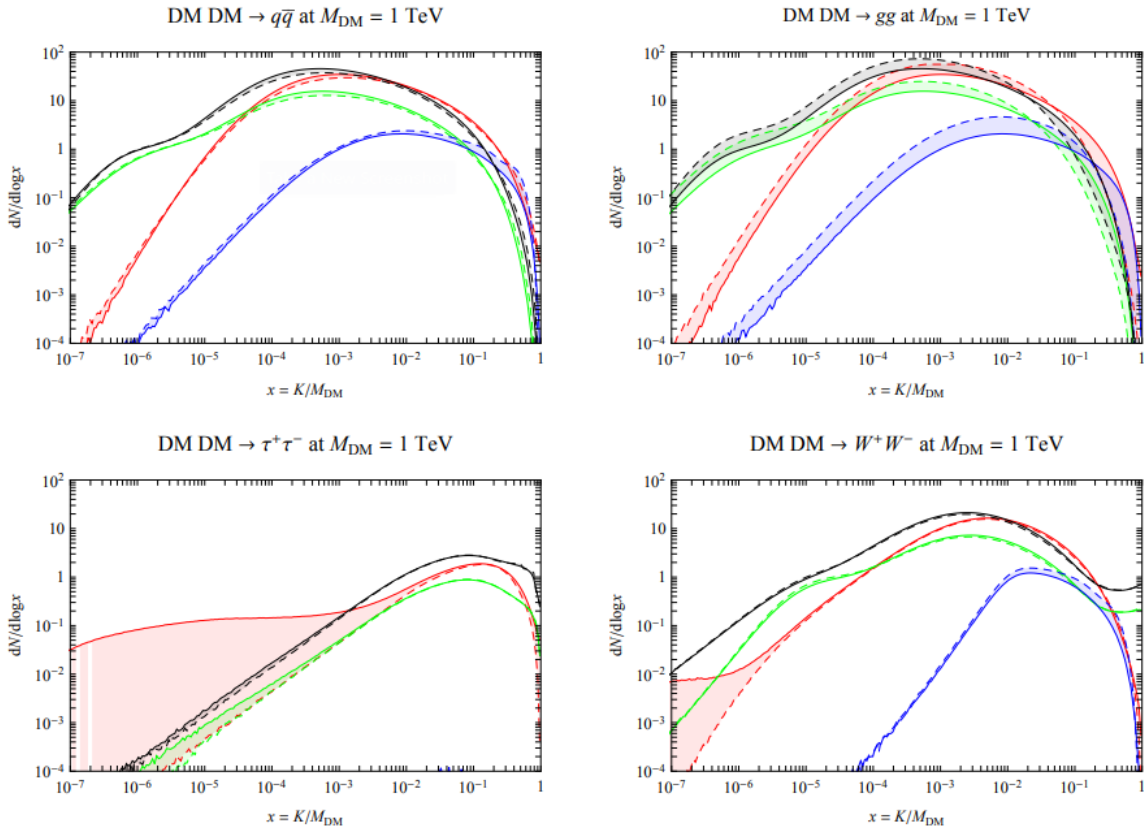


Figure 2.14 Dark Matter annihilation spectra for different final state particle and standard model annihilation channels [24]. Photons (red), e^\pm (green), \bar{p} (blue), ν (black).

408 Exposing our observations to more cosmic messengers greatly increases our sensitivity to rare
 409 processes. In the case of DM, Fig. 2.14, there are many SM particles produced in a dark matter
 410 annihilation. Among the final state fluxes are gammas and neutrinos. Charged particles are also
 411 produced however they would not likely make it to Earth since they will be deflected by magnetic
 412 fields between the source and Earth. This means observatories that can see the neutral messengers
 413 are especially good for DM searches and for combining data for a multi-messenger DM search.

CHAPTER 3

414 MULTIMESSENGER ASTROPHYSICS: DETECTING HIGH ENERGY NEUTRAL 415 MESSENGERS

416 3.1 Introduction

417 **TODO: summarize the chapter** Before the 20th century, all astrophysics observations were
418 optical in nature. We literally only saw things with highly magnified optical observations. Then
419 we discovered cosmic rays. Cosmic rays are charged particles, typically naked protons or H+.
420 This was seen by Victor Hess in 19???. Around the same time we discovered neutrinos from beta
421 decay. Sometime around 1950 we started to build neutrino detectors which were mostly sensitive to
422 neutrinos from the sun. Finally, it was theorized that compact objects like black holes and neutron
423 stars would create waves in space-time when they experience mergers or collisions.

424 In the 21st century, we have developed new observation techniques and detectors that are no only
425 sensitive to these four messengers - photons (**TODO: photon**), neutrinos (**TODO: nu**), Cosmic
426 Rays (CR), and Gravitational Wave (WV) - we're collect high energy versions of these events.
427 For the standard model particles, we're now sensitive to all messengers above the MeV energy
428 range. Additionally, the GW's were sensitive to are in the stellar mass black hole region and above
429 within our galactic neighborhood. This means we're becoming sensitive to the fundamental physics
430 occurring within the universe and we can rely on the universe as a TeV+ particle accelerator. We
431 also have the ability to correlate high energy events across messengers and gain new insights on
432 the processes that occur in our universe.

433 This thesis focuses on very high energy (VHE) gamma rays and neutrinos. These can both be
434 observed through the water cherenkov detection technique altho not exclusively. Methods on how
435 to detect and observe these neutral messengers are discussed Section 3.3 and Section 3.4

436 3.2 Charged Particles in a Medium

437 For high energy gamma-rays and neutrinos, we can exploit the same effect that charged particles
438 have with water. This effect is known as Cherenkov radiation. Cherenkov Radiation occurs when a
439 charged particle, usually electrons (e) or muons (μ), traverse a medium, like water, faster than the

440 speed of light in that medium. This is similar to sonic boom where an object moves through air
441 faster than the speed of sound in air. Cherenkov radiation can therefore be thought of as an 'optic
442 boom'. Many astro-particle physics experiments will use water as the medium as because water
443 has a unique set of properties ideal for charged particle tracking.



Figure 3.1 TODO: Show a nuclear reactor with cherenkov radiation[NEEDS A SOURCE][FACT CHECK THIS]

444 The frequency of light emitted due to cherenkov radiation follows the equation:

$$INSERTCherenkovwavelengthcalcHERE. \quad (3.1)$$

445 The absorption spectra is shown in the following figure:

446 3.3 Photons (γ)

447 3.4 Neutrinos (ν)

448 3.5 Opportunities to Combine for Dark Matter



Figure 3.2 TODO: absorption spectrum of liquid and solid water[NEEDS A SOURCE][FACT CHECK THIS]

449

CHAPTER 4

HIGH ALTITUDE WATER CHERENKOV (HAWC) OBSERVATORY

450 **4.1 The Detector**

451 **4.2 Events Reconstruction and Data Acquisition**

452 **4.2.1 G/H Discrimination**

453 **4.2.2 Angle**

454 **4.2.3 Energy**

455 **4.3 Remote Monitoring**

456 **4.3.1 ATHENA Database**

457 **4.3.2 HOMER**

CHAPTER 5

ICECUBE NEUTRINO OBSERVATORY

459 **5.1 The Detector**

460 **5.2 Events Reconstruction and Data Acquisition**

461 **5.2.1 Angle**

462 **5.2.2 Energy**

463 **5.3 Northern Test Site**

464 **5.3.1 PIgeon remote dark rate testing**

465 **5.3.2 Bulkhead Construction**

CHAPTER 6

COMPUTATIONAL TECHNIQUES IN PARTICLE ASTROPHYSICS

467 **6.1 Neural Networks for Gamma/Hadron Separation**

468 **6.2 Parallel Computing for Dark Matter Analyses**

CHAPTER 7

GLORY DUCK

CHAPTER 8**NU DUCK**

BIBLIOGRAPHY

- 472 [1] Anne M. Green. “Dark matter in astrophysics/cosmology”. In: *SciPost Phys. Lect.*
 473 *Notes* (2022), p. 37. doi: [10.21468/SciPostPhysLectNotes.37](https://doi.org/10.21468/SciPostPhysLectNotes.37). URL: <https://scipost.org/10.21468/SciPostPhysLectNotes.37>.
- 475 [2] Bing-Lin Young. “A survey of dark matter and related topics in cosmology”. In: *Frontiers*
 476 *of Physics* 12 (Oct. 2016). doi: <https://doi.org/10.1007/s11467-016-0583-4>.
 477 URL: <https://doi.org/10.1007/s11467-016-0583-4>.
- 478 [3] Gianfranco Bertone, Dan Hooper, and Joseph Silk. “Particle dark matter: evidence,
 479 candidates and constraints”. In: *Physics Reports* 405.5 (2005), pp. 279–390. ISSN:
 480 0370-1573. doi: <https://doi.org/10.1016/j.physrep.2004.08.031>. URL:
 481 <https://www.sciencedirect.com/science/article/pii/S0370157304003515>.
- 482 [4] Gianfranco Bertone and Dan Hooper. “History of dark matter”. In: *Rev. Mod. Phys.*
 483 90 (4 Aug. 2018), p. 045002. doi: [10.1103/RevModPhys.90.045002](https://doi.org/10.1103/RevModPhys.90.045002). URL: <https://link.aps.org/doi/10.1103/RevModPhys.90.045002>.
- 485 [5] Fritz Zwicky. “The Redshift of Extragalactic Nebulae”. In: *Helvetica Physica Acta* 6.
 486 (1933), pp. 110–127. doi: [10.5169/seals-110267](https://doi.org/10.5169/seals-110267).
- 487 [6] Vera C. Rubin and Jr. Ford W. Kent. “Rotation of the Andromeda Nebula from a Spectro-
 488 scopic Survey of Emission Regions”. In: *ApJ* 159 (Feb. 1970), p. 379. doi: [10.1086/150317](https://doi.org/10.1086/150317).
- 490 [7] K. G. Begeman, A. H. Broeils, and R. H. Sanders. “Extended rotation curves of spiral galax-
 491 ies: dark haloes and modified dynamics”. In: *Monthly Notices of the Royal Astronomical So-*
 492 *ciety* 249.3 (Apr. 1991), pp. 523–537. ISSN: 0035-8711. doi: [10.1093/mnras/249.3.523](https://doi.org/10.1093/mnras/249.3.523).
 493 eprint: <https://academic.oup.com/mnras/article-pdf/249/3/523/18160929/mnras249-0523.pdf>. URL: <https://doi.org/10.1093/mnras/249.3.523>.
- 495 [8] *Different types of gravitational lenses*. website. Feb. 2004. URL: <https://esahubble.org/images/heic0404b/>.
- 497 [9] P. Tisserand et al. “Limits on the Macho content of the Galactic Halo from the EROS-2
 498 Survey of the Magellanic Clouds”. In: *A&A* 469.2 (2007), pp. 387–404. doi: [10.1051/0004-6361:20066017](https://doi.org/10.1051/0004-6361:20066017). URL: <https://doi.org/10.1051/0004-6361:20066017>.
- 500 [10] Douglas Clowe et al. “A Direct Empirical Proof of the Existence of Dark Matter”. In: *apjl*
 501 648.2 (Sept. 2006), pp. L109–L113. doi: [10.1086/508162](https://doi.org/10.1086/508162). arXiv: [astro-ph/0608407](https://arxiv.org/abs/astro-ph/0608407)
 502 [*astro-ph*].
- 503 [11] Planck Collaboration and N. et. al. Aghanim. “Planck 2018 results I. Overview and the
 504 cosmological legacy of Planck”. In: *A&A* 641 (2020). doi: [10.1051/0004-6361/2018](https://doi.org/10.1051/0004-6361/2018)

- 505 33880. URL: <https://doi.org/10.1051/0004-6361/201833880>.
- 506 [12] Wenlong Yuan et al. “A First Look at Cepheids in a Type Ia Supernova Host with JWST”. In:
507 *The Astrophysical Journal Letters* 940.1 (Nov. 2022). doi: [10.3847/2041-8213/ac9b27](https://doi.org/10.3847/2041-8213/ac9b27).
508 URL: <https://dx.doi.org/10.3847/2041-8213/ac9b27>.
- 509 [13] Wendy L. Freedman. “Measurements of the Hubble Constant: Tensions in Perspective”. In:
510 *The Astrophysical Journal* 919.1 (Sept. 2021), p. 16. doi: [10.3847/1538-4357/ac0e95](https://doi.org/10.3847/1538-4357/ac0e95).
511 URL: <https://dx.doi.org/10.3847/1538-4357/ac0e95>.
- 512 [14] Jodi Cooley. “Dark Matter direct detection of classical WIMPs”. In: *SciPost Phys. Lect.
513 Notes* (2022), p. 55. doi: [10.21468/SciPostPhysLectNotes.55](https://doi.org/10.21468/SciPostPhysLectNotes.55). URL: <https://scipost.org/10.21468/SciPostPhysLectNotes.55>.
- 515 [15] “Search for new phenomena in events with an energetic jet and missing transverse momentum
516 in pp collisions at $\sqrt{s} = 13$ TeV with the ATLAS detector”. In: *Phys. Rev. D* 103
517 (11 July 2021), p. 112006. doi: [10.1103/PhysRevD.103.112006](https://doi.org/10.1103/PhysRevD.103.112006). URL: <https://link.aps.org/doi/10.1103/PhysRevD.103.112006>.
- 519 [16] *Jetting into the dark side: a precision search for dark matter*. website. July 2020. URL:
520 <https://atlas.cern/updates/briefing/precision-search-dark-matter>.
- 521 [17] Celine Armand et. al. “Combined dark matter searches towards dwarf spheroidal galaxies
522 with Fermi-LAT, HAWC, H.E.S.S., MAGIC, and VERITAS”. In: *Proceedings of Science*.
523 Vol. 395. Mar. 2022. doi: <https://doi.org/10.22323/1.395.0528>.
- 524 [18] Tracy R. Slatyer. “Les Houches Lectures on Indirect Detection of Dark Matter”. In: *SciPost
525 Phys. Lect. Notes* (2022), p. 53. doi: [10.21468/SciPostPhysLectNotes.53](https://doi.org/10.21468/SciPostPhysLectNotes.53). URL:
526 <https://scipost.org/10.21468/SciPostPhysLectNotes.53>.
- 527 [19] Christian W Bauer, Nicholas L. Rodd, and Bryan R. Webber. “Dark matter spectra from
528 the electroweak to the Planck scale”. In: *Journal of High Energy Physics* 2021.1029-8479
529 (June 2021). doi: [https://doi.org/10.1007/JHEP06\(2021\)121](https://doi.org/10.1007/JHEP06(2021)121).
- 530 [20] Riccardo Catena and Piero Ullio. “A novel determination of the local dark matter density”.
531 In: *Journal of Cosmology and Astroparticle Physics* 2010.08 (Aug. 2010), p. 004. doi:
532 [10.1088/1475-7516/2010/08/004](https://doi.org/10.1088/1475-7516/2010/08/004). URL: <https://dx.doi.org/10.1088/1475-7516/2010/08/004>.
- 534 [21] B. P. Abbott et al. “Observation of Gravitational Waves from a Binary Black Hole Merger”.
535 In: *Phys. Rev. Lett.* 116 (6 Feb. 2016), p. 061102. doi: [10.1103/PhysRevLett.116.061102](https://doi.org/10.1103/PhysRevLett.116.061102). URL: <https://link.aps.org/doi/10.1103/PhysRevLett.116.061102>.
- 537 [22] R. Abbasi et. al. “Observation of high-energy neutrinos from the Galactic plane”. In: *Science*
538 380.6652 (June 2023), pp. 1338–1343.

- 539 [23] NASA Goddard Space Flight Center. *Fermi's 12-year view of the gamma-ray sky*. website.
540 2022. URL: <https://svs.gsfc.nasa.gov/14090>.
- 541 [24] Marco Cirelli et al. “PPPC 4 DM ID: a poor particle physicist cookbook for dark matter
542 indirect detection”. In: *Journal of Cosmology and Astroparticle Physics* 2011.03 (Mar.
543 2011), p. 051. DOI: [10.1088/1475-7516/2011/03/051](https://doi.org/10.1088/1475-7516/2011/03/051). URL: <https://dx.doi.org/10.1088/1475-7516/2011/03/051>.
544